

Evolution of the Optical Absorption Spectra and Electronic Structure of the VBO_3 Crystal under High Pressures

N. V. Kazak^{a,*}, A. G. Gavriiliuk^{b,c}, S. G. Ovchinnikov^{a,d}, I. S. Lyubutin^b,
I. S. Edel'man^a, and V. V. Rudenko^a

^a Kirensky Institute of Physics, Siberian Branch, Russian Academy of Sciences, Akademgorodok, Krasnoyarsk, 660036 Russia
*e-mail: nat@iph.krasn.ru

^b Shubnikov Institute of Crystallography, Russian Academy of Sciences, Leninskiĭ pr. 59, Moscow, 119333 Russia

^c Institute for High Pressure Physics, Russian Academy of Sciences, Troitsk, Moscow oblast, 142190 Russia

^d Siberian Federal University, Svobodny pr. 79, Krasnoyarsk, 660041 Russia

Received March 10, 2009

Abstract—The evolution of optical absorption spectra of the ferromagnetic semiconductor VBO_3 under high pressures up to 70 GPa has been investigated. It has been revealed that, below the fundamental absorption edge ($E_{g1} = 3.02$ eV), the spectra exhibit a series of bands V1 (2.87 eV), V2 (2.45 eV), V3 (1.72 eV), and V4 (1.21 eV) due to the $d-d$ transitions in the V^{3+} ion and charge-transfer excitations. A model of the electronic structure of the VBO_3 semiconductor has been constructed. This model combines the one-electron description of the s and p states of boron and oxygen and the many-electron description of the vanadium d states.

PACS numbers: 74.62.Fj, 75.50.-y, 81.40.Tv, 71.27.+a

DOI: 10.1134/S1063776109090118

1. INTRODUCTION

Transition metal borates of the general formula M^{3+}BO_3 ($\text{M}^{3+} = \text{Ti}, \text{V}, \text{Cr}, \text{Fe}$) crystallize in a calcite structure and have a rhombohedral structure with symmetry group $R\bar{3}c(D_{3d}^6)$. Metal ions are located inside oxygen octahedra. Boron and oxygen ions form planar trigonal anions $(\text{BO}_3)^{3-}$, which are arranged in parallel planes alternating with planes containing metal ions. The unit cell involves two formula units. The magnetic properties are determined by the 90° indirect exchange. The majority of the borates exhibit dielectric properties, which are governed by the strong Coulomb repulsion U at the site. Owing to the “Coulomb” nature of the dielectric gap in these systems, there can arise conditions $U < W$ (where W is the width of the d band) at high pressures when the electron correlations are suppressed and the system undergoes an insulator–metal transition. This transition is accompanied by a sharp change in the magnetic properties.

The FeBO_3 compound is a prominent representative of the borate class. This material has a spontaneous magnetic moment at room temperature and, simultaneously, is transparent in the visible spectral range [1–3]. At normal pressure, the FeBO_3 borate is an antiferromagnet with a weak ferromagnetism ($T_N = 348$ K) and an insulator with an optical gap of 2.95 eV. The investigations of the magnetic [4, 5], optical, and electrical [6] properties and the structure [7] of FeBO_3

crystals under high pressures have revealed electronic, magnetic, and structural transitions in the range of approximately 50 GPa. The studies of the Mössbauer effect [4, 5], optical absorption spectra [8], and electrical resistance [6] have demonstrated that the collapse of the magnetic moment at the pressure $P = 46$ GPa [4, 5] is accompanied by an insulator–semiconductor electronic transition with a drastic shift of the optical absorption edge from approximately 3.0 to 0.8 eV [6, 8]. X-ray structural investigations have revealed a structural phase transition at the pressure $P \approx 53$ GPa with a jump in the unit cell volume by 9% [7]. In our previous papers [8–10], we proposed a model of the band structure of the FeBO_3 compound in which the one-electron description of the s and p states of boron and oxygen is combined with the many-electron description of the Fe d states. According to this model, the collapse of the magnetic moment in the FeBO_3 borate is associated with the crossover of the high-spin (HS, $S = 5/2$) and low-spin (LS, $S = 1/2$) terms of the Fe^{3+} ion with an increase in the crystal field Δ due to an increase in the pressure. It has been shown that, in the case of the spin crossover, the effective Hubbard parameter U_{eff} strongly depends on the pressure, which leads to a weakening of the correlation effects and can result in an insulator–metal transition.

Unlike the ferromagnetic insulator FeBO_3 , the vanadium borate VBO_3 at normal pressure is a ferromagnetic semiconductor [11] with the Curie tempera-

Table 1. Lattice parameters of borate crystals (r_i is the effective ionic radius taken from [14])

$M^{3+}BO_3$	$r_i, \text{Å}$	$r_i^3, \text{Å}^3$	$a_H, \text{Å}$	$c_H, \text{Å}$	c_H/a_H	$V, \text{Å}^3$
VBO ₃	0.640	0.262	4.621	14.516	3.14	268.4
FeBO ₃	0.645	0.268	4.524	14.470	3.13	267.9

ture $T_C = 34$ K and the relatively high activation energy $E_a = 0.92$ eV [12]. At high pressures, the optical absorption was measured in our recent work [13].

In this work, the evolution of optical absorption spectra of VBO₃ single crystals under high pressures up to 70 GPa has been thoroughly investigated and a model of the electronic structure that explains the experimentally observed optical transitions has been constructed.

2. SAMPLE PREPARATION AND EXPERIMENTAL TECHNIQUE

Single crystals of the VBO₃ compound were grown using solution–flux crystallization in the V₂O₃–B₂O₃–(70 wt % PbO + 30 wt % PbF₂) system. The technique used for preparing samples was described in detail in our earlier work [11]. This technique made it possible to produce single crystals in the form of hexagonal thin plates to approximately $1.5 \times 1.5 \times 0.1$ mm³ in size with a smooth lustrous surface. The crystals were transparent and brown in color. The C₃ optic axis was perpendicular to the plate plane.

The crystal structure was investigated at room temperature on a D8 ADVANCE powder automated diffractometer equipped with a Vantec detector (CuK_α radiation, $\lambda = 1.5406$ Å, scan range $2\theta = 13.4^\circ$ – 89.7°). The measurements have revealed the rhombohedral symmetry group $R\bar{3}c(D_{3d}^6)$. The lattice parameters of the VBO₃ crystals are presented in Table 1. For comparison, the data obtained for FeBO₃ crystals are also presented in Table 1. It can be seen that the closeness of the ionic radii r_i of the V³⁺ and Fe³⁺ cations makes it possible to prepare isostructural crystals with close values of the lattice parameters.

Two plates with different thicknesses were chosen for the measurements in a high-pressure chamber [13]. The thin plate had sizes of approximately 20×40 μm² and a thickness $d \approx 1$ – 2 μm, and the thick plate had sizes of approximately 40×40 μm² in the plane and a thickness $d \approx 10$ – 15 μm.

The optical absorption spectra were measured in the pressure range from 1.3 to 69.5 GPa at room temperature in the chamber with diamond anvils. The anvil diameter was equal to 350 μm, and the diameter of a hole in the rhenium gasket for the samples was approximately equal to 200 μm. The PÉS-5 polyethylsiloxane fluid providing quasi-hydrostatic conditions of compression served as a pressure-transmitting

medium. The pressure was measured using the conventional technique based on a shift in the ruby fluorescence line. For this purpose, several ruby crystals up to 10 μm in size were placed in the working volume of the chamber in the vicinity of the samples under investigation. The photographs of the experimental assembly in the high-pressure chamber with diamond anvils at three pressures (7.8, 35.1, 69.5 GPa) are displayed in Fig. 1.

The optical absorption spectra were measured in the visible and near-IR ranges (from 0.4 to 1.9 μm) at room temperature [13]. A photomultiplier (FÉU-100) was used as a detector in the visible range. In the near-IR range, light was detected by a germanium diode cooled to the liquid-nitrogen temperature. A light beam from a halogen lamp was focused on the sample in the direction perpendicular to the plate plane. The diameter of the light spot on the sample was approximately equal to 20 μm. In order to eliminate possible spurious signals, the reference signal I_0 outside the sample was measured initially and then the signal passed through the sample was detected. The optical absorption was calculated from the Bouguer law $I = I_0 \exp(-\alpha d)$, where α is the optical absorption coefficient and d is the sample thickness.

3. EVOLUTION OF THE OPTICAL ABSORPTION SPECTRA UNDER HIGH PRESSURE

The characteristic optical absorption spectra of the thin and thick samples of the VBO₃ crystals at different pressures are shown in Figs. 2a and 2b, respectively.

At low pressures, the absorption spectra of the thin sample exhibit a band with an energy $E > 3$ eV. The low-energy edge of this band at 3.02 eV determines the fundamental absorption edge E_{g1} of the VBO₃ crystals. This energy is close to an energy of 2.95 eV determined for the FeBO₃ compound [1]. As the pressure increases to $P = 27.7$ GPa, the edge slightly shifts toward the high-energy range, which corresponds to an increase in the band gap. This is most likely associated with the change in the band shape with an increase in the pressure. Such a pressure dependence of the band gap E_g was also revealed for the FeBO₃ compound (see Fig. 3).

Below the absorption edge, it is possible to distinguish two broad bands with different intensities in the energy ranges $E \approx 2.87$ eV (band V1) and $E \approx 2.45$ eV (band V2) (see Table 2). With an increase in the pres-

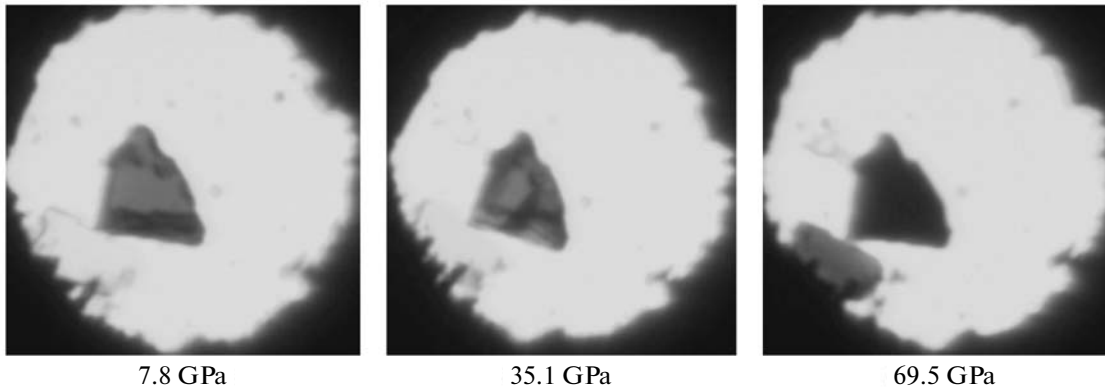


Fig. 1. Micrographs of the VBO_3 crystals in the working volume of the high-pressure chamber at pressures of 7.8, 35.1, and 69.5 GPa (the diameter of the bright spot is approximately equal to 100 μm). The thick sample is dark brown in color at low pressures and black in color at the maximum pressure (the dark crystal in the figure). The thin sample is light yellow in color at low pressures and cherry in color at the maximum pressure (the light crystal in the figure). One of the ruby crystals is seen near the thick sample.

sure, the intensity of the V2 band rapidly increases by a factor of approximately four with a change in the pressure from 1.3 to 27.7 GPa. It should be noted that the intensity of the V1 band depends weakly on the pressure. At a pressure $P_c \approx 30$ GPa, the absorption coefficient in the range $E > 2.5$ eV increases drastically. This effect appears as a shift in the optical absorption edge to 2.25 eV. With a further increase in the pressure, the energy of the optical gap monotonically decreases and reaches a value of 1.92 eV at the pressure $P = 69.5$ GPa.

The absorption spectra of the thick sample have a complex shape (Fig. 2b). The absorption strongly increases in the vicinity of $E \approx 2.4$ eV. Most likely, this portion of the spectrum is a left shoulder of the V2 band, which in the thick sample forms the edge of the “fictive” absorption at the energy $E_{g2} \approx 1.8$ eV. As the pressure increases to $P \approx 30$ GPa, the energy of this edge increases and reaches a value close to the energy of the fundamental absorption edge E_{g1} for the thin sample (Figs. 2a, 3). In the pressure range 30 GPa $< P < 55$ GPa, the fictive absorption edge E_{g2} for the thick sample shifts toward the low-energy range at a rate approximately identical to the rate of the shift in the absorption edge E_{g1} for the thin crystal (Figs. 2, 3). With an increase in the pressure, a new absorption band at $E \approx 1.72$ eV (band V3) manifests itself for the thick sample. The intensity of this band slowly increases in the range $P < 20$ GPa. The low-energy edge of the V3 band with an energy $E \approx 1.5$ eV forms the absorption edge E_{g3} . After passage through the critical pressure P_c , the intensity of the V3 band rapidly increases and the energy of the edge E_{g3} decreases to 1.1 eV. With a further increase in the pressure, the optical gap slowly narrows down and the edge shifts toward the low-energy range and reaches $E \approx 0.94$ eV at the maximum pressure $P = 69.5$ GPa.

We approximated the experimental data in the vicinity of the absorption edge formed by the V3 band with the use of the expression $\alpha E = A(E - E_g)^m$, where A is the constant; $m = 1/2$ and $3/2$ for the allowed and forbidden direct transitions, respectively; and $m = 2$ and 3 for the allowed and forbidden indirect transitions. The processing shows that the best agreement is achieved under the assumption that the V3 band is attributed to the forbidden direct interband transitions.

It is interesting to note that the narrow absorption band at $E \approx 1.21$ eV, which was observed in the absorption spectra of the VBO_3 compound in our previous work [11] at normal pressure, begins to manifest itself in the spectra under investigation for the thick sample only at pressures $P > 40$ GPa. Probably, this is associated with the interference phenomena on the surface of the single crystals. The interference maxima are clearly seen in the absorption spectra of the thick sample at low pressures. An increase in the pressure leads to an increase in the interference period, and, at $P > 20$ GPa, the maxima become difficultly distinguishable.

The pressure dependences of the fundamental absorption edges for the VBO_3 and FeBO_3 crystals are plotted in Fig. 3. Two absorption edges can be distin-

Table 2. Energies of the optical transitions for the VBO_3 crystal at the pressure $P = 1.3$ GPa (V1–V3) and normal pressure (V4) and their pressure derivatives

Transition	$E(P = 1.3 \text{ GPa}), \text{ eV}$	$dE/dP_{\text{exp}}, \text{ eV/GPa}$	
		$P < P_c$	$P > P_c$
V1	2.87	−0.0023	
V2	2.45	+0.0106	
V3	1.72	−0.013	−0.0095
V4	1.21		−0.0013

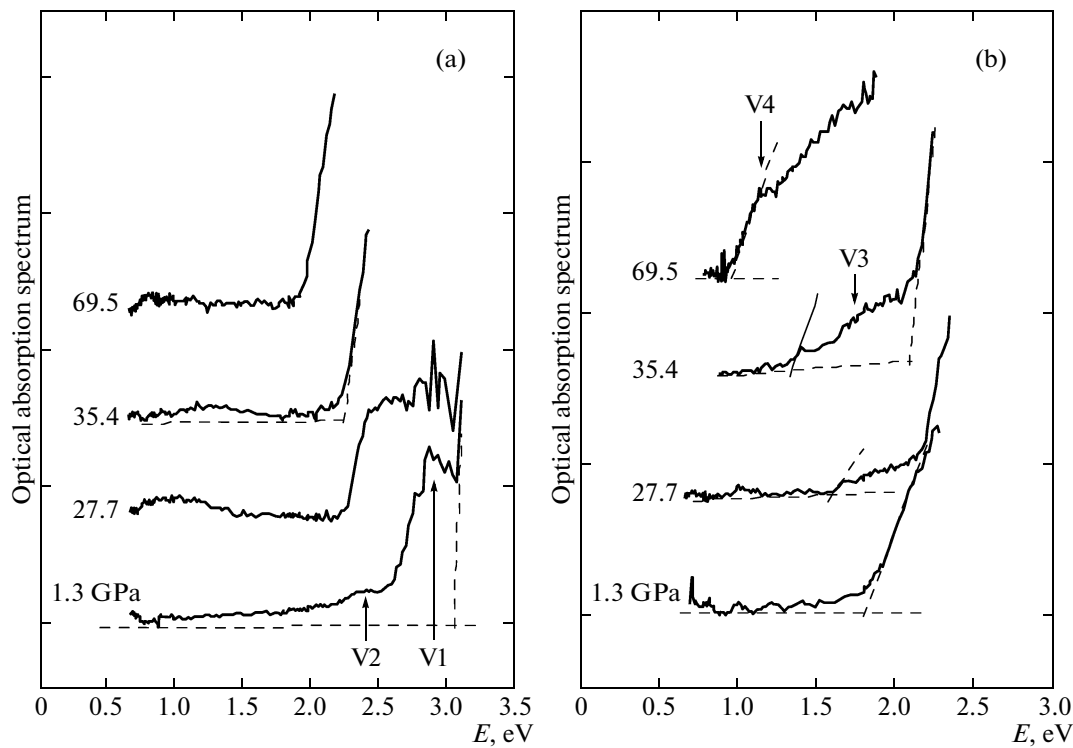


Fig. 2. Evolution of the optical absorption spectrum measured under different pressures at room temperature for (a) thin and (b) thick VBO_3 single-crystal samples.

guished for the vanadium borate: the fundamental absorption edge E_{g1} at $E \approx 3$ eV associated with the fundamental absorption in the thin sample and the absorption edge E_{g3} formed by the V3 band at high pressures in the thick sample. At the critical pressure $P_c \approx 30$ GPa, the optical band narrows down by 0.8 eV in the thin sample and to 0.4 eV in the thick sample; in this case, the absorption edge becomes sharp. The observed electronic transition can be caused by the structural phase transition accompanied by the jump in the unit cell volume. The revealed optical defects (possibly, cracks) arising in the thick sample in passing through the critical pressure (Fig. 1b) count in favor of the possible structural transition [13].

It should be noted that, above and below the electronic transition, the optical spectra vary in a monotonic manner. At $P > 30$ GPa, the energies of both absorption edges decrease linearly with the pressure. The approximation of the pressure dependence of the optical gap by a linear function allowed us to estimate the pressure P_m at which the gap vanishes and the complete metallization takes place [13]. The corresponding estimates are as follows: $P_m = 293 \pm 20$ GPa for the absorption edge E_{g1} and $P_m = 260 \pm 50$ GPa for the absorption edge E_{g3} . It should also be noted that the pressure P_m determined for the VBO_3 crystal exceeds the corresponding pressure obtained from the estimates of the thermally activated gap for the FeBO_3 crystal ($P_m = 210$ GPa) [6].

4. DISCUSSION OF THE EXPERIMENTAL DATA

Let us consider the absorption spectra of the VBO_3 crystal at a low pressure ($P = 1.3$ GPa). Inside the optical gap, there are two groups of bands V1 with an energy of 2.87 eV ($23\,200\text{ cm}^{-1}$) and V2 with an energy of 2.45 eV ($19\,800\text{ cm}^{-1}$) associated with the weak partially allowed $d-d$ transitions in the V^{3+} ion. The investigations of the absorption spectra of $\text{Fe}_{1-x}\text{V}_x\text{BO}_3$ ($x = 0.30, 0.18, 1.00$) solid solutions at different temperatures have revealed a low-intensity temperature-independent peak at an energy $E \approx 9800\text{ cm}^{-1}$ [11]. This band is designated as V4. In order to compare the absorption bands with the energy spectrum of the vanadium borate, we use the Tanabe–Sugano diagram [15], which represents the level splitting of an ion with the d^2 electronic configuration in the crystal field Δ with the cubic symmetry (Fig. 4).

Earlier [11], the V4 band was attributed to the first spin-allowed $d-d$ transition ${}^3T_1(t_2^2) - {}^3T_2(t_2e)$. In this case, it is reasonable to assign the V2 band (19800 cm^{-1}) and the V1 band (23200 cm^{-1}) to the allowed transitions from the ground term 3T_1 to the lower excited terms ${}^3T_1(t_2e)$ and ${}^3A_2(e^2)$, respectively. The V4 band should be clearly seen in the absorption spectra against the background of the V2 band, because the band width is proportional to the slope of the curve $E = f(\Delta)$ in the diagram. It can be seen from Fig. 2b that the V4

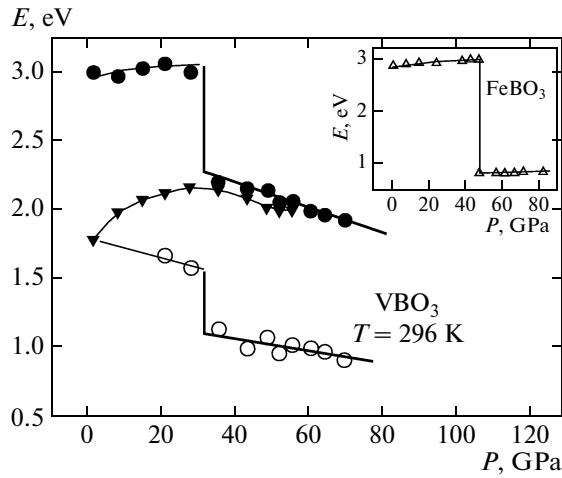


Fig. 3. Pressure dependences of (●) the fundamental absorption edge E_{g1} for the thin VBO_3 sample, (▼) the fictive absorption edge E_{g2} for the thick VBO_3 single crystal, and (○) the absorption edge E_{g3} for the thick VBO_3 single crystal. The inset shows (△) the pressure dependence of the fundamental absorption edge E_g for the FeBO_3 single crystal [6].

band begins to manifest itself in the absorption spectra of the thick sample only at high pressures and is not observed in the absorption spectra of the thin sample. With allowance made for the experimental data obtained, the assumption made in [11] regarding the nature of the V4 band most likely should be rejected. Probably, the V4 band (9800 cm^{-1}) is associated with the low-intensity forbidden $d-d$ transition. The intensity of this band is determined by the statistical probability of the transition that is proportional to the number of absorbing centers and, hence, to the volume of the sample.

We assume that the V4 absorption band is associated with the forbidden $d-d$ transition ${}^3T_1 - {}^1T_2(t_2^2)$ or ${}^1E(t_2^2)$. The width of this band should be small, and its energy should not depend on the crystal field strength, which is observed in the experiment. The values obtained for the Racah parameter $B = 653 \text{ cm}^{-1}$ and the cubic crystal field strength $Dq = 1143 \text{ cm}^{-1}$ are characteristic of V^{3+} ions in the octahedral environment. The crystal field $\Delta = 1.42 \text{ eV}$ for the vanadium borate is close to the crystal field $\Delta = 1.57 \text{ eV}$ determined for the iron borate [8].

The pressure dependence of the position of the V4 band is shown in Fig. 5. In the high-pressure phase ($P > P_c$), this band slowly shifts toward the low-energy range. It can be seen from Fig. 5 that, at $P = 0$, the energy of the V4 band corresponds to the experimentally determined value approximately equal to 1.22 eV .

As can be seen from Fig. 2a, the intensity of the V1 transition is higher than that of the V2 transition. The high intensity of the V1 band can be explained by the

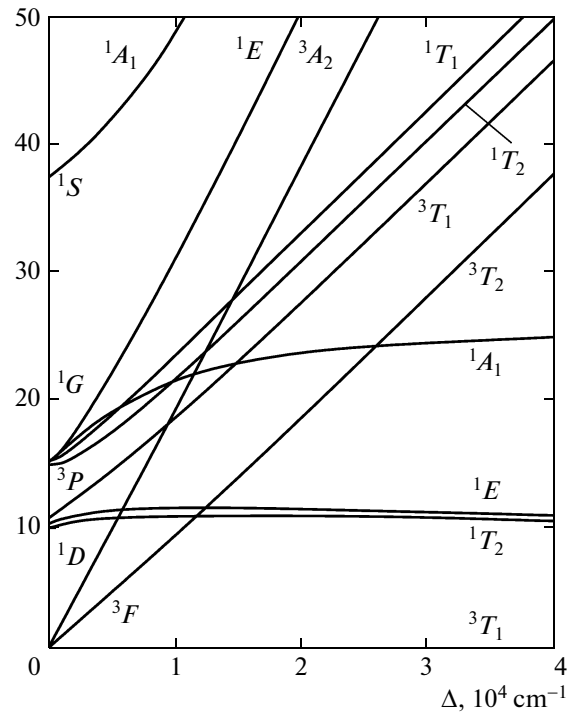


Fig. 4. Tanabe–Sugano diagram of the energy levels for the d^2 electronic configuration in the octahedral crystal field for the parameters $B = 700 \text{ cm}^{-1}$ and $C/B = 4.5$.

additional contribution of the $p-d$ charge-transfer transitions to this band. The intensity of the V2 band depends substantially on the pressure. A variation in the interatomic distances with pressure leads to a variation in the overlap integral between the wave functions, to an increase in the quantum transition probability, and, correspondingly, to an increase in the absorption coefficient.

The absorption spectrum of the thick sample contains the third broad band V3 (at 1.72 eV). The intensity of this band depends strongly on the pressure, and, at $P > P_c$, the low-energy edge of the V3 band determines the absorption edge E_{g3} for the thick sample (Fig. 2a). According to the Tanabe–Sugano diagram, the ground and excited terms do not intersect in the energy range under consideration. The influence of the high pressure can result in a reduction of crystal lattice symmetry and, hence, in an additional splitting of the doubly degenerate term 1T_2 .

5. THE MANY-ELECTRON MODEL OF THE BAND STRUCTURE OF THE VBO_3 CRYSTAL

For FeBO_3 crystals, the one-electron first-principles band calculations within the framework of the local spin density functional theory (the local spin density approximation) [16], in the generalized gradient approximation (GGA) [17] accounting for the

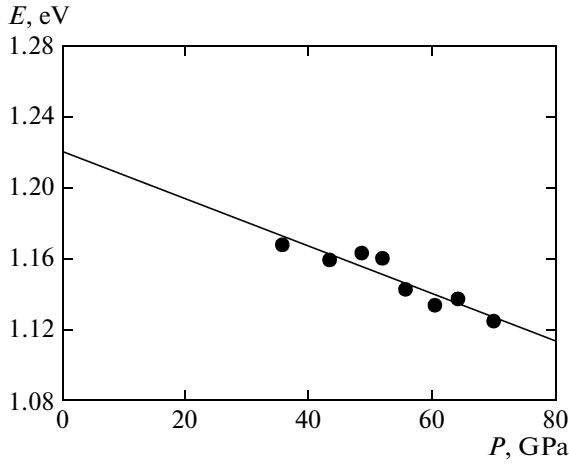


Fig. 5. Pressure dependence of the energy position of the V4 absorption band for the VBO₃ single crystal in the high-pressure phase.

nonlocal corrections to the local density approximation, and within the GGA + U approach [18] have revealed the following specific features of the electronic structure. The conduction band ε_C is predominantly formed by the B *s* and B *p* states, and the top of the valence band ε_V , for the most part, is formed by the O *s* and O *p* states. In the antiferromagnetic phase, the gap between the conduction and valence bands is approximately equal to 2.5 eV and close to the energy of the experimentally observed optical absorption edge. There is a strong hybridization inside the BO₃ group. The overlap of the O *s* and O *p* orbitals with the Fe *d* orbitals is small. This leads to a decrease in the *d*–*d* interatomic hopping integral *t* as compared to that for typical 3*d* metal oxides.

The calculations of the molecular orbitals of finite clusters VB₆O₆ and FeB₆O₆ [11] have demonstrated that the strongly hybridized *s* and *p* states of the BO₃ group hardly depend on the type of the magnetic ion and we can assume that the bottom of the conduction band ε_C and the top of the valence band ε_V for the VBO₃ crystal are close to those for the FeBO₃ crystal and that the separation between them (absorption threshold) is $E_g = \varepsilon_C - \varepsilon_V \approx 3$ eV. In this case, the absorption edge is determined by the electric dipole transitions from the filled valence band to the conduction band.

In view of the strong electron correlations, the band structure of the VBO₃ crystal can be considered within the multiband Hubbard model, which includes *d* states of cations, *s* and *p* states of anions, and local Coulomb interactions in terms of the generalized tight-binding method. This method (cluster perturbation theory) was first proposed for calculating high-temperature superconducting cuprates [19] and, more recently, within the simplified version, for FeBO₃ crystals [20] and Fe_{1-x}V_xBO₃ solid solutions [21]. In this section, we propose a more general description of the

electronic structure with due regard for the excited states of the V³⁺ ion and interatomic hoppings as compared to that in [20, 21].

Inside the gap, the *d* states of a cation are described by the Hamiltonian

$$H_{am} = \sum_{\lambda\sigma} \left(\varepsilon_{\lambda} n_{\lambda\sigma} + \frac{U_{\lambda}}{2} n_{\lambda\sigma} n_{\lambda\bar{\sigma}} \right) + \frac{1}{2} \sum_{\substack{\lambda, \lambda' \\ (\lambda \neq \lambda')}} \sum_{\sigma\sigma'} (V_{\lambda\lambda'} n_{\lambda\sigma} n_{\lambda'\sigma'} - J_{\lambda\lambda'} a_{\lambda\sigma}^+ a_{\lambda\sigma} a_{\lambda'\sigma'}^+ a_{\lambda'\sigma'}), \quad (1)$$

where $n_{\lambda\sigma} = a_{\lambda\sigma}^+ a_{\lambda\sigma}$, $a_{\lambda\sigma}$ stands for the operator of creation of a *d* electron in one of the five orbitals λ with the spin projection σ , and $\bar{\sigma} = -\sigma$. The first term describes the *d* atomic levels in the crystal field. We ignore the uniaxial component of the crystal field and set $\varepsilon(t_{2g}) = \varepsilon_d - 2\Delta/5$ and $\varepsilon(e_g) = \varepsilon_d + 3\Delta/5$. The other terms in relationship (1) correspond to the intraorbital Coulomb repulsion U_{λ} , interorbital Coulomb repulsion $V_{\lambda\lambda'}$, and the Hund's exchange $J_{\lambda\lambda'}$. For simplicity, we disregard the orbital dependence of the Coulomb matrix elements and consider that there are three parameters *U*, *V*, and *J* related to each other by the known relationship following from the spherical symmetry of the atom: $U = 2V + J$.

Figure 6 shows the diagram of the ground and nearest excited energy levels of the terms *d*¹, *d*², and *d*³ with the spin *S*. The energies of the terms are given in Table 3. For the *d*¹ and *d*² configurations, the corresponding wave functions and their energies are elementarily written. For the *d*³ configuration, the wave function of the term with the maximum spin 3/2 and $S_z = 3/2$ is represented in the form $3/2|d^3, 3/2\rangle = d_{1\uparrow}^+ d_{2\uparrow}^+ d_{3\uparrow}^+ |\text{vac}\rangle$ with the energies listed in Table 3. Here, the indices 1, 2, and 3 correspond to different *d* orbitals and |vac⟩ indicates the vacuum state *d*⁰. For the *d*³ configuration with the spin $S = 1/2$, one of the three degenerate (with respect to the orbital moment) configurations has the form

$$\left| d^3, \frac{1}{2} \right\rangle = \frac{1}{2\sqrt{2}} \quad (2)$$

$$\times (2d_{1\uparrow}^+ d_{2\uparrow}^+ d_{3\downarrow}^+ - d_{1\uparrow}^+ d_{2\downarrow}^+ d_{3\uparrow}^+ - d_{1\downarrow}^+ d_{2\uparrow}^+ d_{3\uparrow}^+) |\text{vac}\rangle.$$

It is easy to demonstrate that the Hund's exchange term in Hamiltonian (1) gives zero contribution for the state $|d^3, 1/2\rangle$.

The order of the excited terms of the *d*² and *d*³ configurations is determined by the relationships between the parameters of the Hund's exchange *J* and the crystal field Δ ; that is,

$$E_0(2) - E_1^1(2) = 2J - \Delta, \quad (3)$$

$$E_{1/2}(3) - E_{3/2}^1(3) = 4J - \Delta. \quad (4)$$

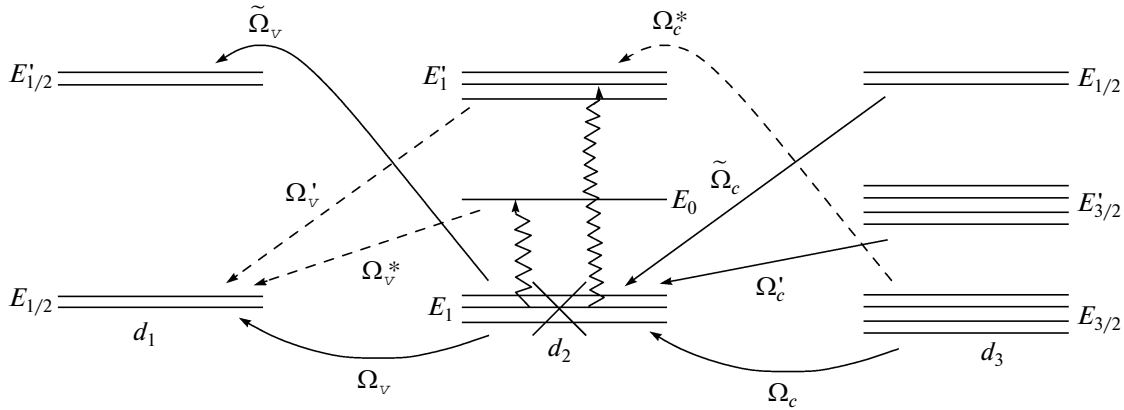


Fig. 6. Energy scheme of the ground and low-lying excited levels $E_S(d^n)$ with spin S for $n = 1, 2,$ and 3 . The cross shows the filled term of the V^{3+} ion. Arrows identify local Fermi quasiparticles with the energies $\Omega_{ij} = E_i(d^{n+1}) - E_j(d^n)$. Solid (dashed) arrows indicate excitations with nonzero (zero) spectral weights.

The Hund's exchange parameter J can be obtained from the optical data: the difference between the energies of the ground term 3T_1 and the forbidden term 1T_2 determines the energy of the V4 band (9800 cm^{-1}) and is $E({}^1T_2) - E({}^3T_1) = 2J$; as a result, we find $J = 0.6 \text{ eV}$. This value is rather close to the parameter $J = 0.7 \text{ eV}$ typical of iron. The order of the excited levels (Fig. 6) follows from the conditions $2J < \Delta$ and $4J > \Delta$.

The annihilation of an electron in the generalized tight-binding method is described by a set of quasiparticles, i.e., the excitations between the terms $d^{n+1} \rightarrow d^n$ and $d^n \rightarrow d^{n-1}$ (shown by the arrows in Fig. 6). The excitations $d^3 \rightarrow d^2$ are designated by the index c , because the upper Hubbard band for a Mott–Hubbard insulator is similar to the conduction band for a conventional insulator. By analogy with the valence band, the excitations $d^2 \rightarrow d^1$ are designated by the index v . The quasiparticle energies $\Omega_{ij} = E_i(d^{n+1}) - E_j(d^n)$ have a one-particle meaning and can be represented in the one-electron band diagram and the density of one-particle states $N(E)$.

The Hubbard X -operators $X^{pq} = |p\rangle\langle q|$ provide an adequate mathematical language for the description of excitations of the Bose type (excitons) and the Fermi

type between the levels $|p\rangle$ and $|q\rangle$ with the energy $\Omega_{pq} = E_p - E_q$. In the X -operator representation, the local Green's function of the d electrons with Hamiltonian (1) can be exactly calculated and has the form [22]

$$D_{pq}(E) = \langle\langle X^{pq} | X^{+pq} \rangle\rangle_E = \frac{F(p, q)}{E - \Omega_{pq} + i\delta}. \quad (5)$$

Here, $F(p, q) = \langle X^{pp} \rangle + \langle X^{qq} \rangle$ is the occupation factor, which is referred to as the end factor in the diagram technique [23]. It is this occupation factor that fundamentally differs the many-electron concept from the one-electron concept. Owing to this factor, the excitations between two unoccupied levels have zero spectral weight. These excitations are termed the virtual excitations, which can acquire nonzero spectral weight in deviations from the stoichiometry, occupation of excited terms at high temperatures, or external pumping. The virtual excitations Ω'_v , Ω_v^* , and Ω_c^* are shown by the dashed lines in Fig. 6.

The d – d transitions discussed in Section 4 between the many-electron terms of the ground and excited states of the V^{3+} ion are depicted by the wavy lines in Fig. 6. Only two lower excited terms are shown for

Table 3. Energies $E_S(n)$ of the ground and first excited terms of vanadium ions (the subscript indicates the spin, and n denotes the electronic configuration)

d^1	d^2	d^3
$E_{1/2}(1) = \varepsilon_d - \frac{2}{5}\Delta$	$E_1(2) = 2\varepsilon_d - \frac{4}{5}\Delta + V - J$	$E_{3/2}(3) = 3\varepsilon_d - \frac{6}{5}\Delta + 3V - 3J$
$E'_{1/2}(1) = \varepsilon_d + \frac{3}{5}\Delta$	$E_0(2) = 2\varepsilon_d - \frac{4}{5}\Delta + V + J$	$E'_{3/2}(3) = 3\varepsilon_d - \frac{1}{5}\Delta + 3V - 3J$
	$E'_1(2) = 2\varepsilon_d + \frac{1}{5}\Delta + V - J$	$E_{1/2}(3) = 3\varepsilon_d - \frac{6}{5}\Delta + 3V$

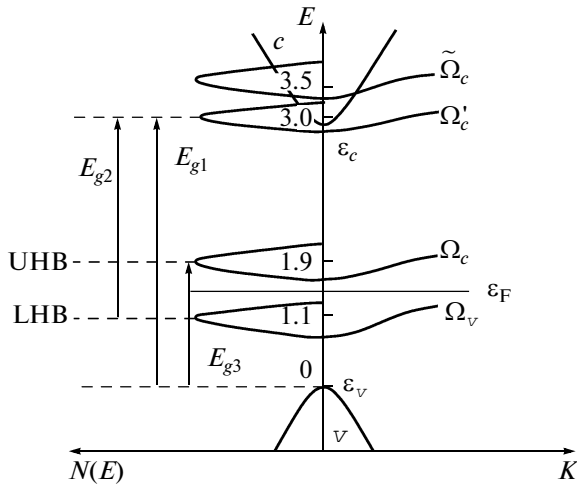


Fig. 7. Schematic diagram of the band structure and optical transitions of the VBO₃ crystal in the absence of an external pressure. Dashed lines indicate the virtual levels Ω_c^* , Ω_v^* , and Ω'_v with zero density of states. The Fermi level lies in the Mott–Hubbard gap between the bands Ω_c and Ω_v . The calculation was performed for the model parameters (11).

simplicity. The energies of these local excitons are calculated from the Tanabe–Sugano diagram and do not depend on the interatomic hoppings.

All Fermi excitations with the filled ground term $E_1(2)$ of the V^{3+} ion as the initial or final state have nonzero spectral weight. Taking into account that, in the paramagnetic state, three spin sublevels of the term $E_1(2)$ are degenerate and that the occupation number of each sublevel is equal to $1/3$, we find $F = 1/3$ for all quasiparticles that are shown by the solid lines with arrows in Fig. 6 and designated as Ω_v , $\tilde{\Omega}_v$, Ω_c , Ω'_c , and $\tilde{\Omega}_c$, where

$$\Omega_c = E_{3/2}(3) - E_1(2) = \varepsilon_d - \frac{2}{3}\Delta + 2V - 2J,$$

$$\Omega_v = E_1(2) - E_{1/2}(1) = \varepsilon_d - \frac{2}{5}\Delta + V - J.$$

The energies of the other local Fermi excitations can be easily written using Table 3.

The addition of interatomic hoppings to Hamiltonian (1), that is,

$$H_t = \sum_{i,j,\sigma} t_{ij} a_{i\lambda,\sigma}^+ a_{j\lambda,\sigma} \quad (6)$$

(where t_{ij} is the matrix element of electron hopping from the i th site to the j th site), leads to the appearance of the dispersion for the Fermi quasiparticles. In the simplest Hubbard–I approximation, which holds true far from the Mott–Hubbard transition, the dispersion law for the band $\Omega_{pq}(k)$ has the form [24] $\Omega_{pq}(k) =$

$\Omega_{pq} - F_{pq}t(k)$, where $t(k)$ is the Fourier transform of the hopping parameter t_{ij} . The presence of the occupation factor ahead of $t(k)$ results not only in the correlation narrowing ($\sim 1/(2S + 1)$) of the band but also in zero dispersion for the virtual excitations.

As a result of the hoppings, the levels Ω_c and Ω_v are smeared into narrow bands of Hubbard fermions and the gap between them represents the Mott–Hubbard gap

$$E_{MH} = \Omega_c - \Omega_v - 2Ft(k=0). \quad (7)$$

In the nearest-neighbor approximation, we have $t(k=0) = zt$, where $z = 6$ is the number of the nearest neighbors with the hopping parameters t . Taking into account that $F = 1/3$, the Mott–Hubbard gap can be written in the form

$$E_{MH} = V - J - 4t. \quad (8)$$

The Fermi level lies inside this gap, so that, according to the classification proposed in [25], the VBO₃ compound belongs to Mott–Hubbard insulators. The diagram of the band structure of the VBO₃ crystal in the absence of external pressure is shown in Fig. 7. The position of the level Ω_c (reckoned from the bottom of the valence band $\varepsilon_v = 0$) was determined from the activation energy for conduction according to the results of the measurements performed in our earlier work [26]. Here, the case in point is the hole conduction at the top of the valence band. The activation energy of the d electrons in the lower Hubbard band is considerably lower than Ω_c ; however, the charge-carrier mobility in the Hubbard band is negligible due to the smallness of the band width. For borates, the typical value of the parameter t determined for the FeBO₃ compound is $t = 0.05$ eV [27]. Since the lattice parameters for the VBO₃ and FeBO₃ crystals are close to each other, we assume that the parameter t for the VBO₃ compound is the same.

Changes in the band structure under pressure are associated with the dependence of the parameters of the crystal field Δ and the hopping t on the distance. Outside the range of first-order structural phase transitions, it is believed that this dependence is linear; that is,

$$\Delta(P) = \Delta(0) + \alpha_\Delta P, \quad t(P) = t(0) + \alpha_t P. \quad (9)$$

6. CHANGE IN THE ELECTRONIC STRUCTURE UNDER HIGH PRESSURE AND COMPARISON WITH EXPERIMENT

According to the proposed model of the band structure, the fundamental absorption edge is determined by the electric dipole transitions v band $\rightarrow c$ band with the energy E_{g1} and this energy should be close to the energy E_g for the FeBO₃ compound. It can be seen from Fig. 3 that, above and below the electronic transition caused by the pressure, the pressure dependences of the energies of the absorption edges for the vanadium borate exhibit a linear behavior

$E_g(P) = E_g(0) + \alpha_{E_g} P$. The magnitude of the energy of the fundamental absorption edge $E_{g1} = 3.02$ eV for the VBO₃ compound is close to the corresponding energy determined for the FeBO₃ borate. A weak increase in the energy of the edge in the pressure range $P < P_c$ is also identical: $\alpha_{E_g} = 0.0015$ eV/GPa.

Above the absorption edge at normal pressure, there are two v band \rightarrow d band excitations $\Omega'_c(k)$ and $\tilde{\Omega}_c(k)$ with the minimum energies $\Omega_c + \Delta - 2t(0)$ and $\Omega_c + 3J - 2t(0)$, respectively. As the pressure increases, the energy of the band $\Omega'_c(k)$ increases and the energy of the band $\tilde{\Omega}_c(k)$ decreases; that is,

$$\tilde{\Omega}_c(P) = \tilde{\Omega}_c(0) - (0.4\alpha_\Delta + 2\alpha_t)P. \quad (10)$$

We believe that the jump in all spectra at $P_c \approx 30$ GPa is associated with the first-order structural phase transition. This transition results in a stepwise increase in the parameters Δ and t dependent on the interatomic distance. As a consequence, the excitation $\tilde{\Omega}_c(P_c)$ appears to be inside the gap E_{g1} and becomes observable. Therefore, at finite pressures, the energy of the edge is determined by $\min(E_{g1}(P), \tilde{\Omega}_c(P))$ and the linear shift in the absorption edge is given by expression (10).

Therefore, the absorption edge at pressures above P_c is formed by the allowed $\varepsilon_v \rightarrow \tilde{\Omega}_c(k)$ at the minimum energy $E'_{g1} = \tilde{\Omega}_c(k=0) = \Omega_c(P) + 3J - 2t(P)$ with the pressure derivative $dE'_{g1}/dP = -(0.4\alpha_\Delta + 2\alpha_t)$. The allowed p - d transition $\varepsilon_v \rightarrow \Omega_c(k)$, which is responsible for the absorption edge E_{g3} , has the energy $E_{g3} = \Omega_c(k=0) = \Omega_c(P) - 2t(P)$. The pressure derivative is $dE_{g3}/dP = -(0.4\alpha_\Delta + 2\alpha_t)$. The edge E_{g2} is assigned to the allowed p - d transition $\Omega_v(k) \rightarrow \varepsilon_c$ from the lower Hubbard d band to the bottom of the conduction band. The energy of this transition is $E_{g2} = \varepsilon_c - \Omega_v(P) + 2t(P)$ with the pressure derivative $dE_{g2}/dP = 0.4\alpha_\Delta + 2\alpha_t$.

The parameters of the electronic structure are determined from the spectra at zero pressure: $E_{g2}(0) = E_{g3}(0) = 1.7$ eV. The energy is reckoned from the top of the valence band. Then, we have $\varepsilon_v = 0$, $\varepsilon_c = 3.0$ eV, $\Omega_v = 1.3$ eV, and $\Omega_c = 1.7$ eV. For these energies, we obtain $U_{\text{eff}} = 0.4$ eV and the Mott–Hubbard gap $E_{\text{MH}} = 0.2$ eV. The observed semiconductor electrical properties of the VBO₃ borate are associated with the smallness of the effective Hubbard parameter and the Mott–Hubbard gap as compared to the effective Hubbard parameter $U_{\text{eff}} = 4$ eV and the dielectric properties of the FeBO₃ borate. Therefore, the final set of the microscopic parameters determined for Hamiltonian (1) from the optical data at zero pressure is as follows:

$$\begin{aligned} \Delta(0) &= 1.42 \text{ eV}, & J &= 0.6 \text{ eV}, \\ V &= 1.0 \text{ eV}, & t(0) &= 0.05 \text{ eV}. \end{aligned} \quad (11)$$

The band structure with the above parameters in the absence of external pressure is schematically shown in Fig. 7. The Fermi level lies inside the Mott–Hubbard gap. Consequently, the refinement of the model in our work with the inclusion of interatomic hoppings and new optical data retains the conclusion drawn in [11] that the VBO₃ compound belongs to the class of Mott–Hubbard insulators.

It should be noted that all signs of the derivatives of the absorption edges E'_{g1} , E_{g2} , and E_{g3} correspond to the experimental data. In terms of the proposed model, the energy of the absorption edge E_{g2} increases linearly with the pressure. The observed nonlinearity is most likely associated with the superposition of several possible excitations with different pressure derivatives in this energy range. In particular, an increase in the pressure is accompanied by an increase in the defect concentration. As a result, some forbidden transitions become allowed and their intensities increase. Generally speaking, the quantities α_Δ and α_t below and above the critical point P_c can be different. Taking into account that the contribution of the interatomic hopping parameter is insignificant, this parameter can be taken to be equal to the corresponding parameter for the FeBO₃ compound: $\alpha_t = 0.00033$ eV/GPa [27]. It follows from the pressure dependence of the V3 band at $P < P_c$ that $\alpha_\Delta = 0.031$ eV/GPa, which is 1.5 times larger than the corresponding parameter determined for the FeBO₃ borate. For these parameters, the edge of the band $\tilde{\Omega}_c$ decreases from 3.4 eV ($P = 0$) to ≈ 3.0 eV ($P = P_c$). In other words, directly before the transition, the bottom of the band $\tilde{\Omega}_c$ drops to the absorption edge E_{g1} .

The first-order structural phase transition is responsible for the jump in the lattice parameters and the model parameters Δ and t dependent on the interatomic distance. Instead of the smooth dependences (9), there are jumps $\delta\Delta = \Delta(P_c + 0) - \Delta(P_c - 0)$ and $\delta t = t(P_c + 0) - t(P_c - 0)$. As a consequence, the bottom of the bands $\Omega_v(k)$, $\Omega_c(k)$, and $\tilde{\Omega}_c(k)$ above the pressure P_c drops abruptly by the same value $D = 0.4\delta\Delta + 2\delta t$. At $P > P_c$, the bottom of the band $\tilde{\Omega}_c(k)$ turns out to be lower than E_{g1} and determines the absorption edge $E'_{g1} = 2.25$ eV at $P = P_c + 0$. As a result, the jump is estimated to be $D = 0.75$ eV. This value is in agreement with the jump in the energy of the absorption edge E_{g1} at the transition point (Fig. 3).

As can be seen from Fig. 3, the pressure derivatives dE'_{g1}/dP and dE_{g3}/dP in the high-pressure phase ($P > P_c$) are considerably smaller than those in the low-pressure phase ($P < P_c$). By using the pressure deriva-

tive of the absorption edge E_{g1}^r at high pressures, we estimated the quantity $\alpha_\Delta = 0.02$ eV/GPa, which almost coincides with the quantity $\alpha_\Delta = 0.018$ eV/GPa for the FeBO_3 compound [8]. According to the theory proposed in this work, the pressure derivatives of both edges should coincide in the pressure range $P > P_c$. The experimental values coincide in the order of magnitude but not quantitatively. The factors responsible for the discrepancy remain unclear, and their elucidation requires the construction of a more detailed and exact theory.

The presence of the virtual levels allows us to expect strong photoinduced effects in optical spectra. In particular, the pumping with the energy $\hbar\omega = \Delta = 1.42$ eV leads to the population of the excited term $E_1^r(d^2)$, which results in the spectral weight of the excitations $\Omega_c^* = E_{3/2}(d^3) - E_{3/2}^r(d^2) = \Omega_c - \Delta$ in the vicinity of 0.37 eV and the excitations $\Omega_v' = E_1^r(d^2) - E_{1/2}(d^1) = \Omega_v + \Delta$ in the vicinity of 2.73 eV. Similarly, the pumping by light with the circular polarization at the energy $\hbar\omega = J = 0.6$ eV leads to the population of the level $E_0(d^2)$, which results in an additional intensity in the absorption spectrum at the energy Ω_v^* in the vicinity of 1.9 eV.

7. CONCLUSIONS

In conclusion, it should be noted that the analysis of the optical absorption spectra of the VBO_3 single crystal has demonstrated that the fundamental absorption edge $E_{g1} = 3.02$ eV for vanadium borate is associated with the electric dipole transitions from the valence band ε_v to the conduction band ε_c and is determined by the strongly hybridized s and p states of the BO_3 group. A series of absorption bands V1–V4 with different intensities lie inside the optical gap. These bands are due to the magnetic dipole transitions in the V^{3+} ion and charge-transfer excitations. At a critical pressure $P_c \approx 30$ GPa, the crystal undergoes an electronic transition accompanied by a drastic change in the optical properties and a narrowing of the optical gap to $E_{g1}^r = 2.25$ eV. The main features of the absorption spectra and their evolution under high pressure have been explained in terms of the many-electron model of the band structure of the VBO_3 crystal with due regard for the one-electron s and p states of boron and oxygen and many-electron terms of the V^{2+} , V^{3+} , and V^{4+} ions. It has been shown that, in the high-pressure phase, the fundamental absorption edge E_{g1}^r is determined by the allowed electric dipole p – d transitions $\varepsilon_v \rightarrow \tilde{\Omega}_c(k)$. The fact that the energy E_{g1}^r does not vanish but takes on a value typical of semiconductors indicates the occurrence of a transition of the

semiconductor–semiconductor type. The critical pressure at which a transition to the metallic state can occur is estimated as $P_m \approx 290$ GPa.

ACKNOWLEDGMENTS

We would like to thank A.D. Vasil'ev for performing the X-ray diffraction investigations.

This study was supported by the Russian Foundation for Basic Research (project nos. 07-02-00490a, 08-02-00897a, 08-02-90708 mob_st, 09-02-00171a, and 07-02-00226), the Federal Agency for Science and Innovation (Rosnauka) (project no. MK-4278.2008.2, contract no. 01.164.12.HB11), and the Branch of Physical Sciences of the Russian Academy of Sciences within the framework of the program “Strongly Correlated Electrons.”

REFERENCES

1. I. S. Édel'man, A. V. Malakhovskii, T. I. Vasil'eva, and V. N. Seleznev, *Fiz. Tverd. Tela (Leningrad)* **14** (9), 2810 (1972) [*Sov. Phys. Solid State* **14** (9), 2442 (1972)].
2. V. N. Zabluda, A. V. Malakhovskii, and I. S. Édel'man, *Fiz. Tverd. Tela (Leningrad)* **27** (1), 133 (1985) [*Sov. Phys. Solid State* **27** (1), 77 (1985)].
3. P. A. Markovin, A. M. Kalashnikova, R. V. Pisarev, and Th. Rasing, *Pis'ma Zh. Éksp. Teor. Fiz.* **86** (11), 822 (2007) [*JETP Lett.* **86** (11), 712 (2007)].
4. I. A. Troyan, A. G. Gavriilyuk, V. A. Sarkisyan, I. S. Lyubutin, R. Ruffer, O. Leupold, A. Barla, B. Doyle, and A. I. Chumakov, *Pis'ma Zh. Éksp. Teor. Fiz.* **74** (1), 26 (2001) [*JETP Lett.* **74** (1), 24 (2001)].
5. A. G. Gavriilyuk, I. A. Trojan, I. S. Lyubutin, S. G. Ovchinnikov, and V. A. Sarkisyan, *Zh. Éksp. Teor. Fiz.* **127** (4), 780 (2005) [*JETP* **100** (4), 688 (2005)].
6. I. A. Troyan, M. Eremets, A. G. Gavriilyuk, I. S. Lyubutin, and V. A. Sarkisyan, *Pis'ma Zh. Éksp. Teor. Fiz.* **78** (1), 16 (2003) [*JETP Lett.* **78** (1), 13 (2003)].
7. A. G. Gavriilyuk, I. A. Trojan, R. Boehler, M. Eremets, A. Zerr, I. S. Lyubutin, and V. A. Sarkisyan, *Pis'ma Zh. Éksp. Teor. Fiz.* **75** (1), 25 (2002) [*JETP Lett.* **75** (1), 23 (2002)].
8. A. G. Gavriilyuk, I. A. Trojan, S. G. Ovchinnikov, I. S. Lyubutin, and V. A. Sarkisyan, *Zh. Éksp. Teor. Fiz.* **126** (3), 650 (2004) [*JETP* **99** (3), 566 (2004)].
9. S. G. Ovchinnikov and V. N. Zabluda, *Zh. Éksp. Teor. Fiz.* **125** (1), 150 (2004) [*JETP* **98** (1), 135 (2004)].
10. S. G. Ovchinnikov, *Zh. Éksp. Teor. Fiz.* **134** (1), 172 (2008) [*JETP* **107** (1), 140 (2008)].
11. N. B. Ivanova, V. V. Rudenko, A. D. Balaev, N. V. Kazak, V. V. Markov, S. G. Ovchinnikov, I. S. Edel'man, A. S. Fedorov, and P. V. Avramov, *Zh. Éksp. Teor. Fiz.* **121** (2), 354 (2002) [*JETP* **94** (2), 299 (2002)].
12. N. V. Kazak, A. D. Balaev, S. G. Ovchinnikov, N. B. Ivanova, and V. V. Rudenko, *J. Magn. Magn. Mater.* **300**, e507 (2006).

13. A. G. Gavriilyuk, N. V. Kazak, S. G. Ovchinnikov, and I. S. Lyubutin, *Pis'ma Zh. Éksp. Teor. Fiz.* **88** (11), 877 (2008) [*JETP Lett.* **88** (11), 762 (2008)].
14. R. D. Shannon, *Acta Crystallogr., Sect. A: Cryst. Phys., Diffr., Theor. Gen. Crystallogr.* **32**, 751 (1976).
15. Y. Tanabe and S. Sugano, *J. Phys. Soc. Jpn.* **9**, 766 (1954).
16. A. V. Postnikov, St. Bartkowski, M. Neumann, R. A. Rupp, E. Z. Kurmaev, S. N. Shamin, and V. V. Fedorenko, *Phys. Rev. B: Condens. Matter* **50**, 14849 (1994).
17. K. Parlinski, *Eur. Phys. J. B* **27**, 283 (2002).
18. S. Shang, Y. Wang, Z.-K. Liu, C.-E. Yang, and S. Yin, *Appl. Phys. Lett.* **91**, 253115 (2007).
19. S. G. Ovchinnikov and I. S. Sandalov, *Physica C (Amsterdam)* **161**, 607 (1989).
20. S. G. Ovchinnikov, *Pis'ma Zh. Éksp. Teor. Fiz.* **77** (12), 808 (2003) [*JETP Lett.* **77** (12), 676 (2003)].
21. N. B. Ivanova, N. V. Kazak, V. V. Markov, S. G. Ovchinnikov, V. V. Rudenko, and M. M. Abd-Elmeguid, *Fiz. Tverd. Tela (St. Petersburg)* **46** (8), 1422 (2004) [*Phys. Solid State* **46** (8), 1462 (2004)].
22. J. C. Hubbard, *Proc. R. Soc. London, Ser. A* **285**, 542 (1965).
23. R. O. Zaitsev, *Zh. Éksp. Teor. Fiz.* **70** (3), 1100 (1976) [*Sov. Phys. JETP* **43** (3), 574 (1976)].
24. V. V. Val'kov and S. G. Ovchinnikov, *Quasiparticles in Strongly Correlated Systems* (Siberian Branch of the Russian Academy of Sciences, Novosibirsk, 2001), p. 277 [in Russian].
25. J. Zaanen, G. A. Sawatzky, and J. W. Allen, *Phys. Rev. Lett.* **55**, 418 (1985).
26. N. V. Kazak, S. G. Ovchinnikov, M. M. Abd-Elmeguid, and N. B. Ivanova, *J. Phys.: Condens. Matter* **17**, S795 (2005).
27. S. G. Ovchinnikov, V. I. Anisimov, I. A. Nekrasov, and Z. V. Pchelkina, *Phys. Met. Metallogr.* **99** (Suppl. 1), S93 (2005).

Translated by O. Borovik-Romanova